

THE TITLE3

Von der Fakultät für Mathematik, Informatik und Naturwissenschaften der RWTH Aachen University zur Erlangung des akademischen Grades eines Doktors der Naturwissenschaften genehmigte Dissertation

vorgelegt von

THE AUTHOR

PREVIOUS QUALIFICATION

aus HOMETOWN

Berichter: Universitätsprofessor Dr. FOO BAR
Universitätsprofessor Dr. BAZ TEST

Datum der mündlichen Prüfung: XX. Month 2018

Diese Dissertation ist auf den Internetseiten
der Hochschulbibliothek online verfügbar.

THE AUTHOR

THE TITLE3

Dissertation in Physik

Rheinisch-Westfälische Technische Hochschule Aachen

III. Physikalisches Institut A

Berichter: Universitätsprofessor Dr. FOO BAR
 Universitätsprofessor Dr. BAZ TEST

Contents

	Page
1 Experimental Setup	3
1.1 The Large Hadron Collider	3
1.2 The Compact Muon Solenoid	5
2 Deep Learning, Normalizing Flows and Invertible Neural Networks	7
2.1 Foundations of Deep Learning and Neural Networks	7
2.1.1 The Universal Approximation Theorem	7
2.1.2 Fully-Connected Neural Networks	7
2.1.3 Activation Functions	8
Bibliography	11

1 Experimental Setup

In this chapter the experimental context of this thesis will be discussed.

1.1 The Large Hadron Collider

The Large Hadron Collider (LHC) is currently the most powerful particle accelerator in the world. Hosted at CERN in Geneva at the Swiss-French border and first put into operation on 10th September 2008, the LHC is designed for proton and heavy lead ion collisions. The machine has gone through several upgrades between the consecutive data-taking phases (Runs) called Long Shutdowns (LS). During these the proton beam energy has been gradually increased from 3.5 TeV to a recently – on the 5th July, 2022 to be precise – achieved energy of 6.8 TeV [1] resulting in a total centre-of-mass (CM) proton-proton collision energy of $\sqrt{s} = 13.6$ TeV. Similarly, the beam intensity has seen an increase from 1.1×10^{11} protons per bunch (ppb) and ~ 200 bunches to a projected $\sim 1.8 \times 10^{11}$ ppb and ~ 2500 bunches [2, 3]. With a theoretical maximum CM energy of $\sqrt{s} = 14$ TeV and instantaneous luminosity of $L = 10 \times 10^{34} \text{ cm}^{-2}\text{s}^{-1}$ it holds the record in these measures among concurring experiments.

As a result of consecutive accelerator upgrades, the collider complex has an impressive and complex pre-accelerator structure as shown in fig. 1.1. Consequently, the proton bunches first go through multiple preparation steps before they get injected into the 27 km tunnel of the LHC where the four main experiments (ALICE, ATLAS, CMS and LHCb) and their interaction points are located.

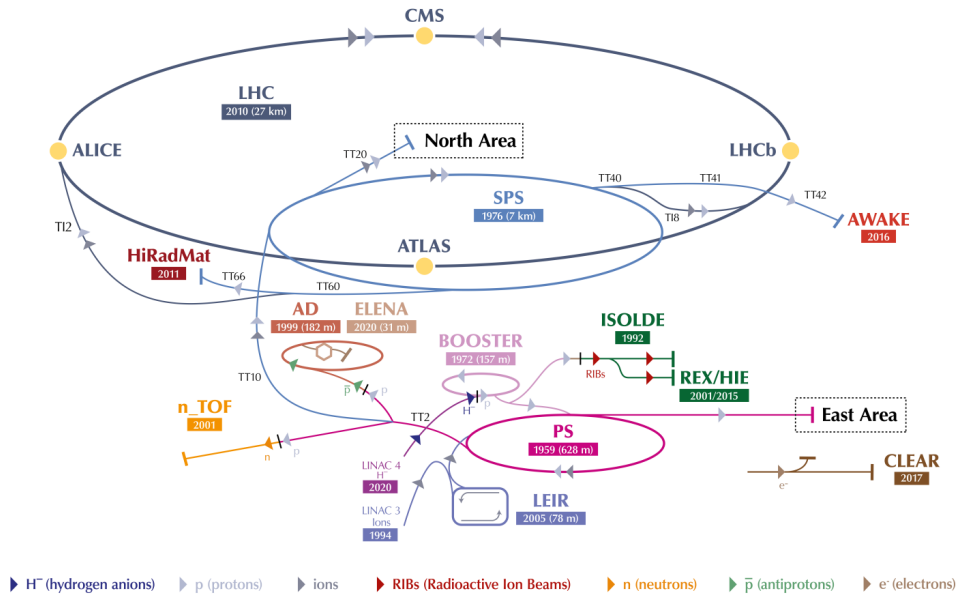


Figure 1.1: The accelerator complex of the LHC, their corresponding construction years and circumferences. Individual stages are shown in different colours, the particle types they accelerate are indicated as arrows. Note that the pre-accelerators do not serve the LHC ring exclusively and the diverging paths lead to other independent experiments. Old tunnels of previous experiments serve as pre-accelerators now in the LHC injection chain. [4]

The four main stages of pre-acceleration for protons are listed in tab. 1.1 below. As proton source, hydrogen is used. The protons are first accelerated in the form of H^- ions through the

86 metre long tunnel of the recently (2020) constructed Linear Accelerator 4 (Linac4). Stripped of their pair of electrons, the protons enter the Proton Synchrotron Booster (PSB) where they reach up to 2 GeV. In the next step of the injection chain, they enter the Proton Synchrotron (PS), historically the first synchrotron at CERN serving exclusively as a pre-accelerator now. Travelling through the 628 metres long ring and accelerated to 26 GeV, the particles are injected into the Super Proton Synchrotron (SPS), where they are awaiting injection into the LHC once they reach 450 GeV.

Accelerator	Peak Energy
Linear accelerator 4 (Linac4)	160 MeV
Proton Synchrotron Booster (PSB)	2 GeV
Proton Synchrotron (PS)	26 GeV
Super Proton Synchrotron (SPS)	450 GeV
Large Hadron Collider (LHC)	7 TeV

Table 1.1: The acceleration chain the protons undergo to reach their final energy of 7 TeV.

In the LHC the beams are circulating in opposing directions. They are kept on a circular trajectory using superconducting NbTi magnets operating at 1.9 K thanks to the superfluid helium bath at about 0.13 MPa [5]. In the tunnel itself there are eight interactions points (IP). ATLAS, ALICE, CMS and LHCb are located at IP1, IP2, IP5 and IP8, respectively. IP3 and IP7 are where to momentum and the betatron collimators located ensuring beam quality; IP4 houses the radiofrequency (RF) cavities bringing the bunches to 7 TeV. IP6 houses the beam dump where old bunches are deflected by the fast-pulsing "kicker" magnets and directed towards the carbon absorber at the end of their lifetime. [6]

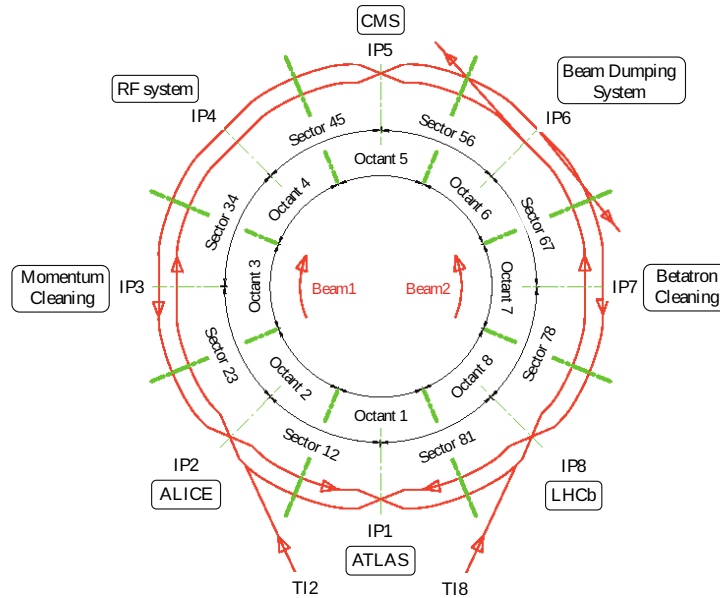


Figure 1.2: The location of the interaction points, the experiments, and the beam adjustment systems. The LHC ring is also divided into further sectors and octants for each IP. [7]

The four main detectors perform the particle collision measurements. LHCb specializes on flavour physics and measures b-quark decays focussing on the measurement and study of CP-violating processes. ALICE has been constructed to mainly study the quark-gluon plasma result-

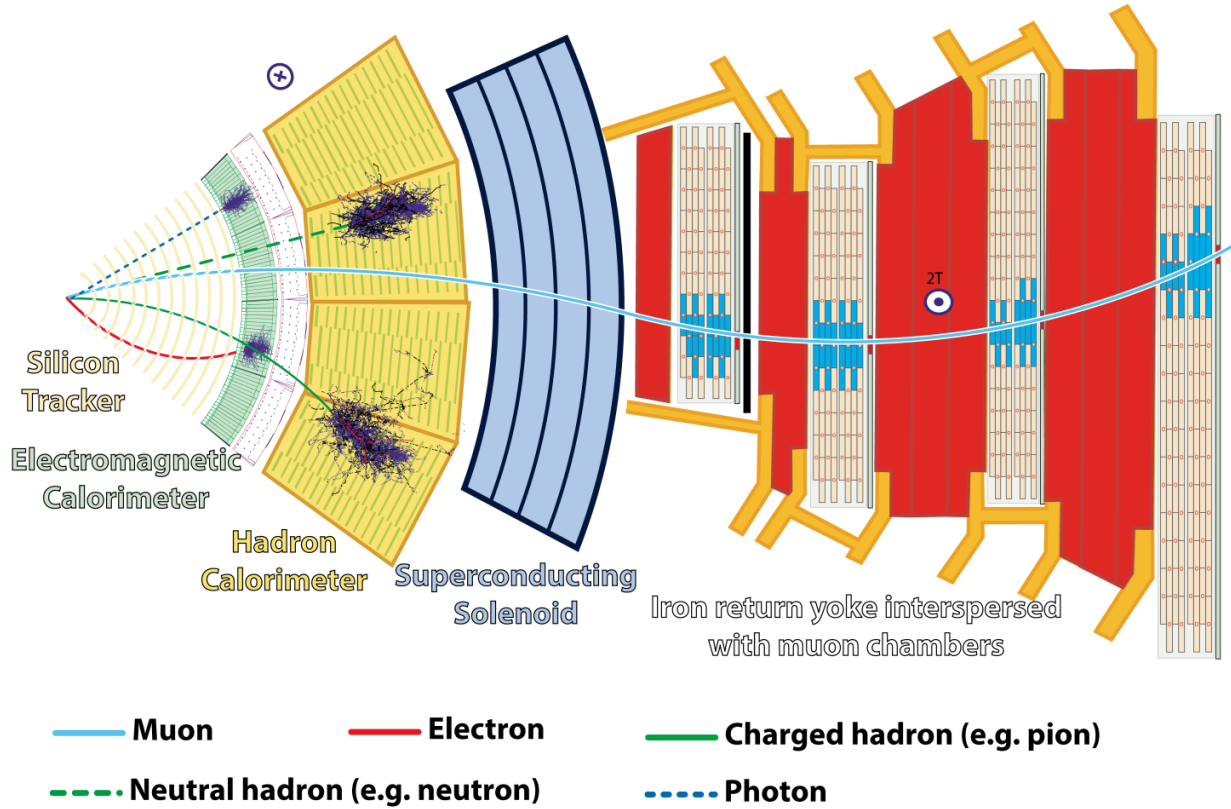


Figure 1.3: from [8]

ing from heavy ion collisions. ATLAS and CMS are sister experiments and are general purpose detectors. In the following, the latter will be described in detail.

1.2 The Compact Muon Solenoid

The Compact Muon Solenoid (CMS) detectors structure is shown in 1.3.

2 Deep Learning, Normalizing Flows and Invertible Neural Networks

Deep Learning is a subdomain within Machine Learning focussing on the construction and training of deep neural networks. Such networks have been proven to be extremely successful in different, analytically unsolvable problems such as (but not restricted to) image classification tasks, regression tasks, image generation tasks, language translation and reinforcement learning. In this chapter, a brief introduction to these networks and their properties with a focus on so-called normalizing flows and invertible neural networks is given.

2.1 Foundations of Deep Learning and Neural Networks

2.1.1 The Universal Approximation Theorem

The success of Neural Networks (NNs) lies in their potential of learning (almost) arbitrary models. This property of NNs can be expressed mathematically through the Universal Approximation Theorem which in words states [9]:

A feed-forward network with linear output and at least one hidden layer with a finite number of nodes can approximate any real continuous function on a given closed and bounded subset to arbitrary precision.

However, the Universal Approximation Theorem does not state how the network should be constructed to achieve the desired precision. For this reason, the theorem has been proven for several network architectures; in case of ReLU-activated feed-forward networks the theorem can be written as the following [10]:

Theorem 1 *For any real and continuous function $f : [0, 1]^{d_{in}} \rightarrow \mathbb{R}^{d_{out}}$ and every $\epsilon > 0$ there is a ReLU-network \mathcal{N} with the same input and output dimension d_{in} and d_{out} and hidden layer width at most w for which*

$$\sup_{x \in [0, 1]^{d_{in}}} \|f(x) - f_{\mathcal{N}}(x)\| \leq \epsilon$$

and

$$d_{in} + 1 \leq w_{min}(d_{in}, d_{out}) \leq d_{in} + d_{out}$$

This theorem does not state anything about the exact depth (number of layers) the network needs to have, its speed of convergence and the optimization process it needs to undergo to achieve this arbitrary approximation. On the other hand, it is reassuring to have a mathematical guarantee for convergence for a given feed-forward network structure. For this reason, empiric studies are usually performed to look for a locally optimal solution for a given task.

In the following, a brief overview of the most common NN components is going to be given with special focus on the ones used for the construction of the cINN.

2.1.2 Fully-Connected Neural Networks

The most elementary NNs perform affine transformations (consisting of a linear transformation represented by a matrix W and a shift b) on a given input x followed by the application of a non-linear function (called activation) g :

$$y = g(Wx + b)$$

Graphically, one such transformation is represented as a layer. For a fully-connected neural network, these transformations are called in succession, resulting in stacked layers of n nonlinearities as shown in fig. 2.1. The resulting mapping

$$f(x, \theta) = g^n \left\{ W^{n-1} g^{n-1} \left[\dots \left(W^2 g^1 (W^1 x + b^1) + b^2 \right) \dots \right] + b^{n-1} \right\}$$

is a universal approximator with the free parameters θ (containing all the matrices W^i and the biases b^i) for the target output for y . Finding the optimal parameters θ is called training and the θ will be referred to as trainable parameters.

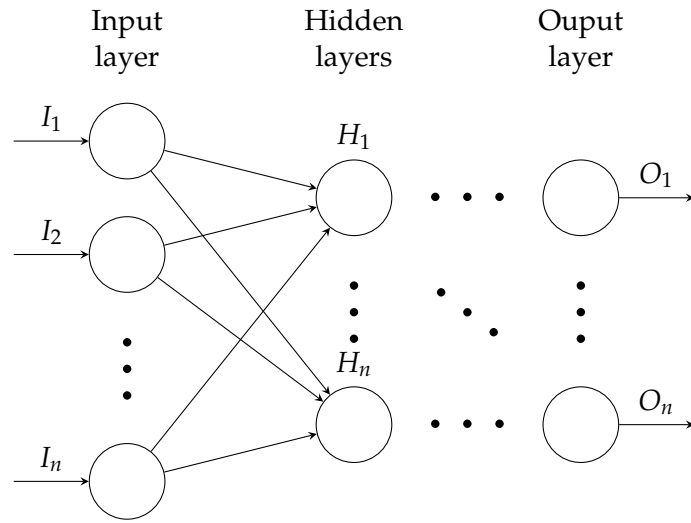


Figure 2.1: Schematic structure of a feed-forward NN. The nodes represent the variables for the hidden and output layers or the biases and the activations g applied to the intermediate outputs for the hidden layers. Arrows represent the matrix W .

Note that for the approximation to work arbitrary well, the structure of the network and training have to be correctly adjusted to the task to be solved.

2.1.3 Activation Functions

It is essential for convergence to select the right activation function g . Historically, several candidate activation functions such as sigmoid, tanh, the rectified linear unit (ReLU) and its variants such as SeLU and leaky-ReLU have emerged. In this work ReLU will be used exclusively. An advantage of ReLU is the lack of saturation range compared to the sigmoid or the tanh activation functions, where gradients above or below a given value of x become negligible, "paralysing" the training. Apart from that, ReLU has tractable derivatives and has proven to be an efficient activator empirically. It is defined as

$$\text{ReLU}(x) = \max\{0, x\}$$

where the maximum is taken element-wise over the vector components of x . Note that its derivative is not continuous and makes a jump at the origin from 0 to 1, which unnecessarily renders

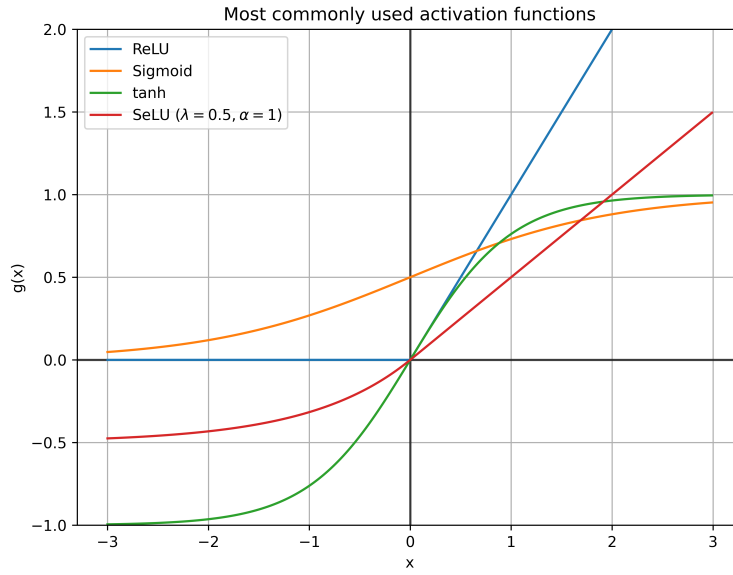


Figure 2.2: Most commonly used activation functions. Note the plateaus of the sigmoid and tanh functions and for all $x < 0$ for ReLU. Setting the gradient zero in case of ReLU for $x < 0$ renders several parameters inactive during training; on the other hand, large positive parameters have do not get stuck due to vanishing gradients and the function is scaleless.

parameters 0 during training. On the other hand, this activation function has no scale, making it an excellent candidate for general approximation tasks. A graph of the most commonly used activation functions is shown in fig. 2.2.

Bibliography

- [1] A. Alici, M. Bomben, I. Dawson, and J. Sonneveld, “The LHC machine and experiments”, (2021). <http://cds.cern.ch/record/2773265>.
- [2] S. Fartoukh, S. Kostoglou, M. Solfaroli Camillocci, G. Arduini, H. Bartosik, C. Bracco, K. Brodzinski, R. Bruce, X. Buffat, M. Calviani, F. Cerutti, I. Efthymiopoulos, B. Goddard, G. Iadarola, N. Karastathis, A. Lechner, E. Metral, N. Mounet, F.-X. Nuiy, P. S. Papadopoulou, Y. Papaphilippou, B. Petersen, T. H. B. Persson, S. Redaelli, G. Rumolo, B. Salvant, G. Sterbini, H. Timko, R. Tomas Garcia, and J. Wenninger, “LHC Configuration and Operational Scenario for Run 3”, tech. rep., CERN, Geneva, Nov, 2021. <https://cds.cern.ch/record/2790409>.
- [3] N. Karastathis, M. Barnes, H. Bartosik, K. Brodzinski, X. Buffat, F. Cerutti, S. Fartoukh, B. Goddard, G. Iadarola, S. L. Naour, A. Lechner, J. M. Heredia, A. Mereghetti, E. Metral, D. Missiaen, N. Mounet, F. X. Nuiy, S. Papadopoulou, Y. Papaphilippou, B. Petersen, G. Rumolo, B. Salvant, C. Schwick, M. S. Camillocci, G. Sterbini, H. Timko, R. T. Garcia, J. Uythoven, and J. Wenninger, “LHC Run 3 Configuration Working Group Report”, (2019). <http://cds.cern.ch/record/2750302>.
- [4] E. Mobs, “The CERN accelerator complex in 2019. Complexe des accélérateurs du CERN en 2019”, (Jul, 2019). <https://cds.cern.ch/record/2684277>. General Photo.
- [5] O. S. Brüning, P. Collier, P. Lebrun, S. Myers, R. Ostojic, J. Poole, and P. Proudlock, *LHC Design Report*. CERN Yellow Reports: Monographs. CERN, Geneva, 2004. <http://cds.cern.ch/record/782076>.
- [6] L. Evans and P. Bryant, “LHC machine”, *Journal of Instrumentation* **3** no. 08, (Aug, 2008) S08001–S08001. <https://doi.org/10.1088/1748-0221/3/08/s08001>.
- [7] C. Bracco, “Commissioning Scenarios and Tests for the LHC Collimation System”, 2009. <http://cds.cern.ch/record/1174254>. Presented on 29 Jan 2009.
- [8] D. Barney, “CMS Detector Slice”, Jan, 2016. <http://cds.cern.ch/record/2120661>. CMS Collection.
- [9] M. Erdmann, J. Glombitza, G. Kasieczka, and U. Klemradt, *Deep Learning for Physics Research*. WORLD SCIENTIFIC, 2021. <https://www.worldscientific.com/doi/pdf/10.1142/12294>. <https://www.worldscientific.com/doi/abs/10.1142/12294>.
- [10] B. Hanin and M. Sellke, “Approximating continuous functions by relu nets of minimal width”, 2017. <https://arxiv.org/abs/1710.11278>.

Selbständigkeitserklärung

Hiermit versichere ich an Eides statt, dass ich diese Arbeit einschließlich evtl. beigefügter Abbildungen, Zeichnungen u.Ä.m. selbstständig angefertigt und keine anderen als die angegebenen Hilfsmittel und Quellen benutzt habe. Alle Stellen, die dem Wortlaut oder dem Sinn nach anderen Werken entnommen sind, habe ich in jedem einzelnen Fall unter genauer Angabe der Quelle deutlich als Entlehnung kenntlich gemacht.

Aachen, den XX. MONTH 2018

THE AUTHOR

Danksagung

Thx.